Design and Manufacture of Resonant Chipless Tags in Millimeter-Wave Band

Raymundo de Amorim, Nicolas Barbot, Romain Siragusa, Christophe Trehoult, Laurent Lyannaz, Etienne Perret

Design and Manufacture of Resonant Chipless Tags in Millimeter Band

Raymundo de Amorim Jr[1], Nicolas Barbot[1], Romain Siragusa[1], Christophe Trehoult[2], Laurent Lyannaz[2] and Etienne Perret[1]
[1]Université Grenoble Alpes, Grenoble INP, LCIS, 26000 Valence, France.
{raymundo.de-amorim-junior,nicolas.barbot,romain.siragusa,etienne.perret}@lcis.grenoble-inp.fr
[2]Centre Technique du Papier, 38400 Saint-Martin-d'Hères, France.

***Abstract*—In this paper, we introduce the first chipless tag in the mmWave band based on resonating elements. One goal is to introduce a millimeter-wave communication system based on chipless tags without a ground plane based on the traditional low-cost printing methods. For this purpose, millimeter-wave chipless resonant tags have been designed considering the trade-offs such as RCS signal level, losses, and design constraints. The proposed design is based on a single layer printing, where each resonating element is replicated to satisfy constraints related to the chipless reading process, at these frequencies. A reading range up to $20\ \mathrm{cm}$ has been noticed in an office environment.**

***Index Terms*—Flexible manufacturing system, Millimeter wave circuit, Chipless RFID tag.**

I. Introduction

The chipless RFID technology is an intermediate technology between the optical and the UHF RFID [1]. A comparison between these 3 technologies is given in Fig. 1. Chipless tags combine some features of the such as a lower cost and some of the UHF RFID. As barcodes, chipless tags are characterized by a low cost since the tag does not use any chip. Instead, the identifier is directly linked to the geometry of the printed elements. As UHF tag, chipless tags can be read independently of the line of sight configuration due to the RF propagation. In this sense, the chipless tags can be seen as a radar target designed to scatter a specific electromagnetic signature. The tag structure is composed basically of metallic ink printed on a substrate, then no additional circuit components are needed. Passive chipless RFID structures fundamentally rely on their RCS, frequency or phase changes to encode the information or some combination of these parameters [2]–[5].

Previous millimeter-wave chipless tags were introduced for chipless RFID applications. Most of these applications are related to the Synthetic Aperture Radar techniques (SAR) [6]–[9], where the dimension of the encoding particle is significantly higher than the wavelength. However, these tags do not behave as resonant scatters. Therefore, the classical information storage based on peak/dip recognition on the spectrum of the backscattered signal cannot be applied to these designs.

In [10] a printed Van-Atta reflectarray structure is analyzed. It is employed for localization purposes, and presents a long detection range $(2.5\ \mathrm{m})$. However, it is not possible to encode sufficient bits when compared to frequency-based tags, within a credit card-sized area for example, which can be considered as a rule of thumb for chipless tags design. Besides, this kind of tag is incompatible with high encoding data capacity. In this article, we propose for the first time a chipless tag operating in the mmWave bandwidth based on resonant scatterers.

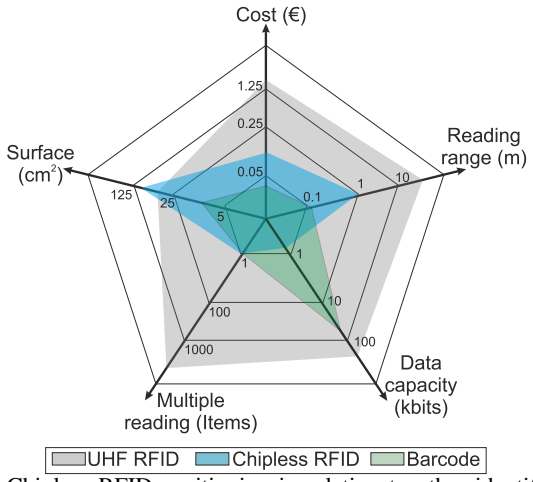

Fig. 1: Chipless RFID positioning in relation to other identification technologies.

Compared to UWB chipless tag, mmWave chipless tag can achieve a better coding capacity and coding density. Furthermore, these tags are less impacted by coupling, since resonant elements may be spaced further apart relative to the wavelength compared to classical designs.

The main goal is to present resonant mmWave chipless tags compatible with the mono-layer printing process. Furthermore, a tag based on a low-cost PET substrate is evaluated, which adds complexity to the system due to the high substrate losses at these frequencies. This approach paves the way to identify tags printed on documents (tag printed directly on bio-sourced material) or even on specific manufactured products.

The next sections of this paper are described as follows. In Section II, the principle of chipless RFID design for mmWave tag is detailed. Section III is dedicated to chipless tag design manufacturing. In Section IV the measurement setup and the results are discussed.

II. Design of resonant chipless tags in millimeter waves

For frequency-based mmWave chipless tags, the most significants parameters are RCS level and the $Q-$factor of the

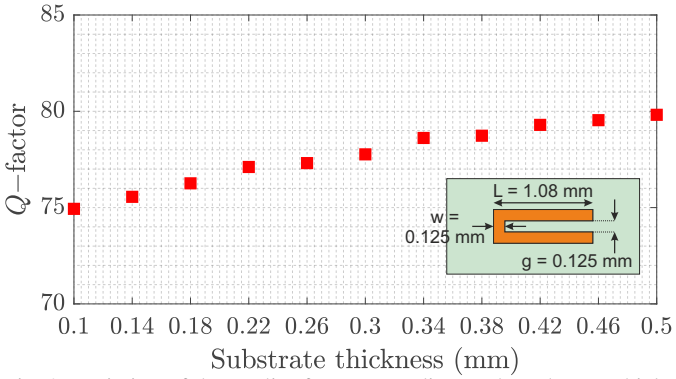

Fig. 2: Variation of the quality factor according to the substrate thickness. All the losses are included with $\epsilon_r = 2.33$, $\tan\delta = 0.009$, copper cladding $t = 50$ μm with conductivity ($\sigma = 5.96 \times 10^7$ S/m).

scatterer. A high backscattered RCS allows the tag to be differentiate from the clutter contributions on which the tag is embedded. The tag $Q-$factor permits isolation by temporal windowing and thus improve the detection of the tag in real environment is related to the frequency band associated with each resonator, which directly determines the number of resonators that belongs to the tag. Then, the design of the tag and therefore of each of these resonators must optimize the RCS and $Q-$factor.

The main drawback in mmWave chipless tag design is related to losses of low cost material used to fabricate the tag. For cost reasons, the manufacturing of tags must also rely on low cost printing processes (flexography, screen printing, inkjet) and commercial inks or additives of dielectric/conductive pigments.

A. Design constraints

An important factor that thoroughly limits the RCS level and quality factor are the manufacturing process limitations, i.e., minimum design conditions that must be respected for the structures fabrication. It is noteworthy that structure without ground plane requires only one conductive layer, which makes it compatible with direct printing processes on the product. Photolithography and inkjet have similar design constraints, the minimum dimension in gap and traces width are limited to 100 μm. For chipless RFID tags, another fundamental characteristic of their design is the presence or absence of a ground plane at the tag structure. Resonators with a ground plane are like resonant cavities, which gives them a high $Q-$factor. The presence of the ground plane also allows good insulation with the object on which they are applied. However, it's difficult to adapt these tags using a printing process on low-cost materials because of the two metal layers' design. Moreover, the RCS is highly impacted due to the quasi-optical reflection originated by the ground plane.

The non-existence of a ground plane generally exposes less marked resonances, which implies in low $Q-$factor. However, it's easier to adapt those tags to a chain process due to its mono-layer characteristic, which relies upon a cost reduction.

B. Losses

In general, the losses undergone in microwave circuits that are built on a substrate are divided into conduction, dielectric, surface, and radiation losses. For mmWave chipless tag, radiation losses become a dominant factor that directly impact the RCS level [11]. Then, the significant reduction of transmitted and backscattered power limits the reader range in chipless mmWave systems to few centimeters (20 cm in office environment). Since the resonator geometry is optimized the dielectric loss, substrate thickness and copper cladding thickness are considered to quality factor assessment. The total quality factor is calculated from the measured resonant frequency (f_0) and the -3 dB bandwidth (Δf) around the resonance frequency. Then, the quality factor is defined as ($Q = f_0/\Delta f$). Considering the copper cladding thickness ($t = 50$ μm), the RCS level and quality factor are driven with the substrate thickness h. A co-planar quarter-wavelength resonator without a ground plane shown in the insets of Fig. 2 is evaluated. Thus, as depicted in Fig. 2, whereas all the losses are embedded in the the model. The total Q-factor is directly proportional to the substrate thickness, that behavior is contrary when microstrip resonators are considered [12].

C. Proof of concept mmWave chipless tags

The RF Encoding Particle (REP) design approach [1] is adopted, and one elementary particle is chosen for encoding information. The first step of that approach is to establish a relation between the geometrical parameters of the isolated scatter and its electromagnetic signature. Well-known tags have been evaluated for resonant mmWave purposes: C-section

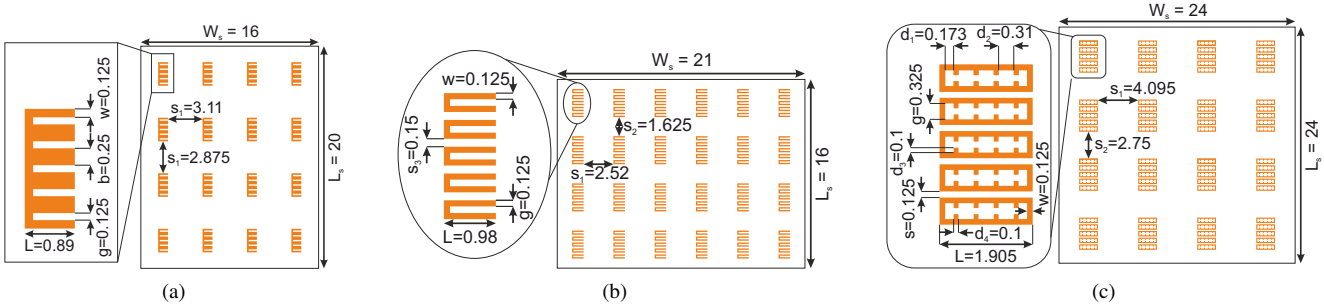

Fig. 3: Design dimensions for the tags without a ground plane. (a) E-shape, (b) C-shape and (c) L-shape. All dimensions are in millimeter.

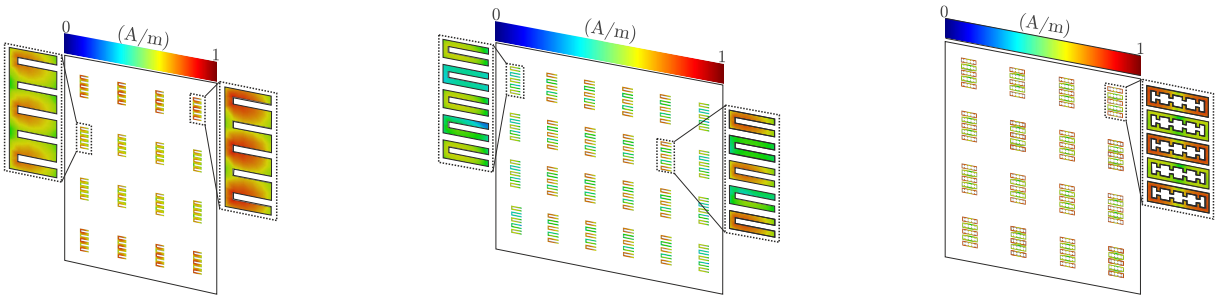

(a) (b) (c)

Fig. 4: Simulated current distributions for the proposed chipless mmWave tags at resonance frequency, (a) E-shape, (b) C-shape and (c) Loop-shape.

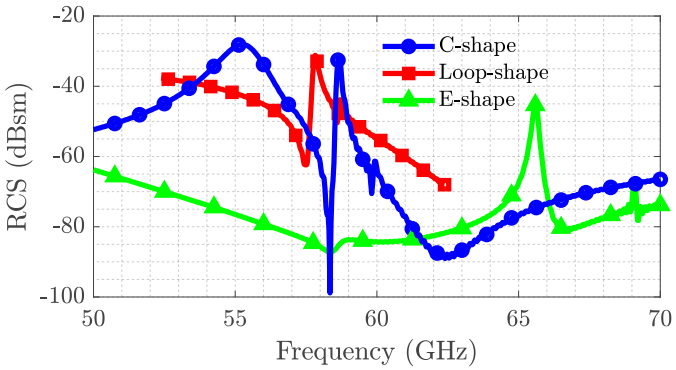

Fig. 5: Simulated RCS as function of frequency for each proposed tag.

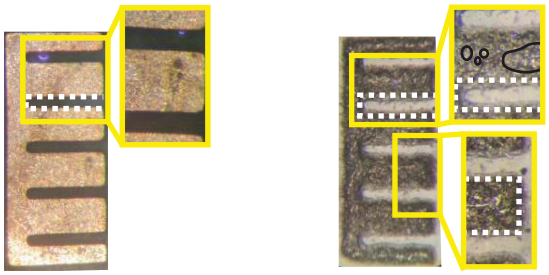

(a) (b)

Fig. 6: E-shape tag without ground plane, (a) low loss material (photolithography) and (a) PET (inkjet). The dotted lines indicate the originally designed tag. The black lines show some imperfections in metallic ink transfer.

[4], Loop-shape [13] and E-shape [14]. The geometrical designs of the tags taking account of the constraints are shown in Fig. 3. Afterward, to overcome the issue related to the tag RCS low backscattered level, each scatterer has been identically replicated to increase the backscattered E-field. The element multiplication does not involve a proportional augmentation to the RCS level, hence an optimization has been performed. The result can be extended to the other structures. The electromagnetic responses of whole structures have been evaluated using CST Microwave Studio. The simulated structure is based on a substrate Rogers RT5880 with $\tan\delta = 0.005$, permittivity $\epsilon_r = 2.33$ and thickness of $h = 0.127$ mm. The curves shown in Fig. 5 correspond to the RCS of the structures and it's respectively surface current at the resonance frequency (see Fig. 4). The backscattered signal is received in co-polarization within the far-field radiation zone. The RCS level for all analyzed structures is higher to -40 dBsm, which allows the tag reading (office environment).

As depicted in Fig. 5 the structures are highly selective and present an RCS that allows the reading even in an office environment. The tag based on E-shape structures have the best trade-off, in terms of size and selectivity. Henceforth, the E-shape structure will be used for applications in low-cost PET substrates.

III. Tags Fabrication

Photolithography realization technology is chosen to realize the tags on low-loss flexible substrates. This process has similar design limitations than in print-based systems. To assess the effectiveness of proposed tags, one-bit frequency information tag from different shapes has been fabricated. It is noteworthy that to design tags with different operating frequencies, the proposed solution can be easily modified. Two substrate have been investigated, the first one is low losses RT5880 (see Fig. 6(a)). The second one is a low cost PET (see Fig. 6(b)), which has a permittivity ($\epsilon_r = 3.5$) and dielectric loss ($\tan\delta = 0.03$) [15]. The PET material offers a good printing but some inconsistencies in the transfer are noticed, as shown in Fig. 6(b) (black lines), it introduces some discontinuities on the design, which can shift the expected frequency and reduced the RCS level.

IV. Experimental Setup and Measurements

The V-band measurements were performed with an Agilent N5222A (10 MHz−26.5 GHz) PNA with Virginia Extensions (VDI modules) to operate from 65 GHz to 72 GHz. The VDI module is a frequency multiplier combined with a mixer with a WR_{15} waveguide output connected to horn antennas on co-polarization configuration. The measurement setup is seen in Fig 7. The tag is positioned on a support made of foam. The tags were placed at distance of 20 cm from the antennas and the bi-static configuration as seen in the insets of the Fig. 7 is used.

The magnitude of S_{21} is shown in Fig. 8 for the tags on RT5880 material and E-shape PET-based substrate. For

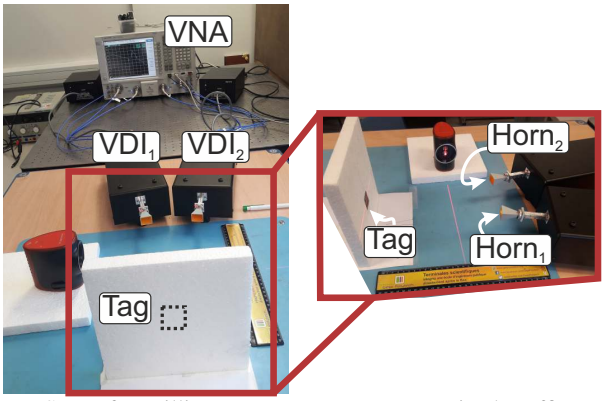

Fig. 7: Setup for millimeter-wave measurements in the office environment. Bi-static configuration is used, and both antennas have a co-polarization orientation.

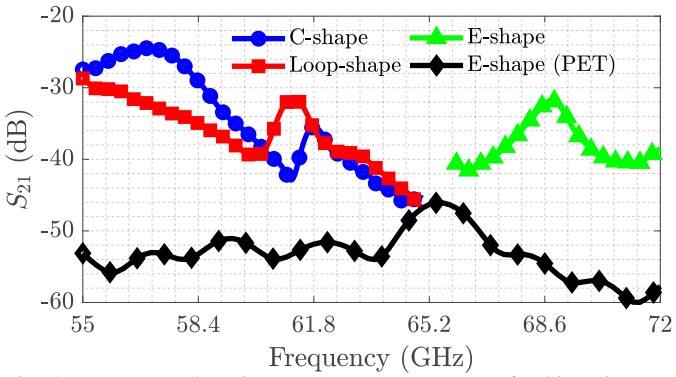

Fig. 8: Frequency domain response measurements for bi-static configuration.

TABLE I: Performance comparison between the chipless tags without ground plane.

	C-shape	L-shape	E-shape	E-shape (PET)
$Q-$factor	73.02	61.92	−80.02	30.72
Resonance peak (dB)	−35.53	−31.48	−31.82	−46.08

each measurement, the tag is removed from the foam and placed in the same position. The resonance can be observed (peak apex) in all cases, which denotes that the backscattered fundamental mode due to the resonant structure is present in all the responses. The EM responses for low-loss tags present a higher RCS when compared to the PET-based tag. Indeed, the losses in PET substrate and metal losses are higher than in the RT5880. A significant frequency shift is seen in E-share PET due to the permittivity and the imperfections generated in the manufacturing process. The RCS and $Q-$factors are resumed in the Table I, as seen in the simulation part, the E-shape presents higher S_{21} level and $Q-$factor.

V. Conclusions

The operating principle of resonant tags for millimeter waves application was evaluated by comparing different designs and different substrate realizations. A prospective study of structures already developed in the UWB band and taken to the millimeter waves band shows that the resonant mmWave tags could be compatible for millimeter waves applications. The constraints on the fabrication process highlight the limitations of the proposed method since a low-cost printing method may be applied. Moreover, these tags have been evaluated without a ground plane, which agrees with low-cost fabrication procedures. The use of the REP approach was analyzed and then the number of resonators were increased. The future work intends to implement a low-cost solution, using bio-based and recyclable techniques from the paper industry.

Acknowledgment

The authors would like to acknowledge the UGA for financially supporting of this project AUSTRALE via the ANR program and European Research Council (ERC) funding under grant agreement N° 772539.

References

[1] E. Perret, *Radio Frequency Identification and Sensors: From RFID to Chipless RFID*. John Wiley & Sons, Dec. 2014.

[2] O. Rance, R. Siragusa, P. Lemaître-Auger, and E. Perret, "Toward RCS Magnitude Level Coding for Chipless RFID," *IEEE Transactions on Microwave Theory and Techniques*, vol. 64, no. 7, pp. 2315–2325, Jul. 2016.

[3] A. Vena, E. Perret, and S. Tedjini, "RFID chipless tag based on multiple phase shifters," in *2011 IEEE MTT-S International Microwave Symposium*, Jun. 2011, pp. 1–4.

[4] ——, "Chipless RFID Tag Using Hybrid Coding Technique," *IEEE Transactions on Microwave Theory and Techniques*, vol. 59, no. 12, pp. 3356–3364, Dec. 2011.

[5] A. Vena, E. Perret, and S. Tedjni, "A Depolarizing Chipless RFID Tag for Robust Detection and Its FCC Compliant UWB Reading System," *IEEE Transactions on Microwave Theory and Techniques*, vol. 61, no. 8, pp. 2982–2994, Aug. 2013.

[6] M. Pöpperl, J. Adametz, and M. Vossiek, "Polarimetric Radar Barcode: A Novel Chipless RFID Concept With High Data Capacity and Ultimate Tag Robustness," *IEEE Transactions on Microwave Theory and Techniques*, vol. 64, no. 11, pp. 3686–3694, Nov. 2016.

[7] M. Zomorrodi and N. C. Karmakar, "Optimized MIMO-SAR Technique for Fast EM-Imaging of Chipless RFID System," *IEEE Transactions on Microwave Theory and Techniques*, vol. 65, no. 2, pp. 661–669, Feb. 2017.

[8] I. Ullmann, K. Root, and M. Vossiek, "Novel Chipless RFID Concept with High Data Capacity," in *2021 IEEE MTT-S International Microwave Symposium (IMS)*, Jun. 2021, pp. 162–164, iSSN: 2576-7216.

[9] L. M. Arjomandi, G. Khadka, and N. C. Karmakar, "mm-Wave Chipless RFID Decoding: Introducing Image-Based Deep Learning Techniques," *IEEE Transactions on Antennas and Propagation*, vol. 70, no. 5, pp. 3700–3709, May 2022.

[10] J. G. D. Hester and M. M. Tentzeris, "Inkjet-Printed Flexible mm-Wave Van-Atta Reflectarrays: A Solution for Ultralong-Range Dense Multitag and Multisensing Chipless RFID Implementations for IoT Smart Skins," *IEEE Transactions on Microwave Theory and Techniques*, vol. 64, no. 12, pp. 4763–4773, Dec. 2016.

[11] R. Garg, I. Bahl, and M. Bozzi, *Microstrip lines and slotlines*. Artech house, 2013.

[12] A. Gopinath, "Maximum Q-Factor of Microstrip Resonators," *IEEE Transactions on Microwave Theory and Techniques*, vol. 29, no. 2, pp. 128–131, Feb. 1981.

[13] R. de Amorim, N. Barbot, R. Siragusa, and E. Perret, "Millimeter-wave Chipless RFID Tag for Authentication Applications," in *2020 50th European Microwave Conference (EuMC)*, Jan. 2021, pp. 800–803.

[14] R. de Amorim, R. Siragusa, N. Barbot, G. Fontgalland, and E. Perret, "Millimeter Wave Chipless RFID Authentication Based on Spatial Diversity and 2-D Classification Approach," *IEEE Transactions on Antennas and Propagation*, vol. 69, no. 9, pp. 5913–5923, Sep. 2021.

[15] H. Suzuki and T. Kamijo, "Millimeter-Wave Measurement of Complex Permittivity by Perturbation Method Using Open Resonator," *IEEE Transactions on Instrumentation and Measurement*, vol. 57, no. 12, pp. 2868–2873, Dec. 2008.